Effect of Ba content on initial magnetization of $Sr_{2-x}Ba_xFeMoO_6$ and the structural stability under high pressure

R. C. Yu,[1,*] P. Zhao,[1] F. Y. Li,[1] Z. X. Liu,[1] J. Liu,[2] and C. Q. Jin[1]

[1]*Laboratory of Extreme Conditions Physics, Institute of Physics, Beijing High Pressure Research Center, Chinese Academy of Sciences, Beijing 100080, People's Republic of China*

[2]*Institute of High Energy Physics, Chinese Academy of Sciences, Beijing 100039, People's Republic of China*

(Received 2 January 2003; revised manuscript received 3 December 2003; published 3 June 2004)

Series samples of $Sr_{2-x}Ba_xFeMoO_6$ have been synthesized using conventional solid-state reaction, and the effect of Ba content on the initial magnetizations of the samples has been studied. The measured saturation magnetizations of the samples show that the degree of antisite of Fe and Mo decreases with increasing Ba content. Structural stability and electrical properties of two samples of $Sr_{2-x}Ba_xFeMoO_6$ under high pressure at room temperature have been studied using energy dispersive x-ray diffraction with synchrotron radiation and resistance and capacitance measurements. The x-ray diffraction results show that the structures of $Sr_{2-x}Ba_xFeMoO_6$ remain stable in the measured pressure range of about 0–40 GPa. The equations of state of the two samples are obtained from the V/V_0-P relationship based on the Birch-Murnaghan equation. The bulk moduli B_0 of the two samples are calculated according to the Birch-Murnaghan equation assuming that their first order derivatives B_0' are equal to 4. The electrical resistance for the samples shows an abrupt drop at about 2.3–3.8 GPa, which might be caused by a change in the electronic structure induced by high pressure.

DOI: 10.1103/PhysRevB.69.214405 PACS number(s): 61.50.Ks, 62.50.+p, 75.47.Gk, 61.10.Nz

I. INTRODUCTION

Since the discovery of the colossal magnetoresistance (CMR) phenomenon in doped perovskite manganese oxides, those materials have attracted a great deal of interest due to their magnetic and electrical properties. Recently, polycrystalline Sr_2FeMoO_6 with an ordered double perovskite structure[1] has drawn considerable attention because of its CMR effect at room temperature. Due to the application prospect of the CMR effect at room temperature, many investigations have been carried out for materials, such as Ca_2FeMoO_6, Ba_2FeMoO_6, and $Sr_{2-x}Ba_xFeMoO_6$, with the same structure as Sr_2FeMoO_6. Sr_2FeMoO_6 consists of alternating FeO_6 and MoO_6 octahedra in the lattice, forming a double perovskite structure. Sr_2FeMoO_6 is known as a ferrimagnet metal with a very high ferromagnetic transition temperature.[1] Each B-site sublattice of $Fe^{3+}(3d^5)$ and $Mo^{5+}(4d^1)$ is considered to arrange ferromagnetically, while the two sublattices are coupled antiferromagnetically. The $3d^5$ electrons of Fe^{3+} ions are localized showing local spin moment $S=5/2$ while the $4d^1$ electrons of Mo^{5+} occupy the conduction band showing spin moment $S=1/2$ in the opposite direction.[1] Up until now, there is still uncertainty about the mechanism for the magnetic interaction in this compound. The saturation magnetization value reported in Ref. 1 suggests the configuration of either $3d^5(Fe^{3+})$ and $4d^1(Mo^{5+})$ or $3d^6(Fe^{2+})$ and $4d^0(Mo^{6+})$. Many groups have done research on magnetism for this compound.[2–7] Mössbauer spectroscopy studies[5] gave more reliable information of Fe^{3+} configuration. The configuration of $Fe^{2+}Mo^{6+}$ should be given with great care since the compound is a metal. Some neutron diffraction measurements[3] gave $0.5\mu_B$ for Mo while some[2] reported zero for it. Considering the electronic itineracy of Mo spin-down t_{2g} electrons it is compellent to explain the saturation magnetization and the conductivity of the compound. Besides these, the cationic disorder of the Fe and Mo sites with a few percent might also play a significant role in the nature of the magnetism.[8,9] An electronic energy calculation[1,10] predicts that Sr_2FeMoO_6 has a half-metallic band structure where the conduction electrons are highly spin-polarized even at room temperature. The results show that the occupied up-spin band comes mainly from Fe $3d$ electrons. The Fermi level exists within the spin-down band, which is composed of Fe t_{2g} and Mo t_{2g} electrons. The electrons of Fe and Mo cations may be considered as localized and itinerant, respectively, with the valence states of $Fe^{3+}(3d^5;t_{2g}^3e_g^2,S=5/2)$ and $Mo^{5+}(4d^1;t_{2g}^1,S=1/2)$. The magnetoresistance has been considered to be associated with electron tunneling through an insulating barrier formed at the grain boundaries. The antiferromagnetic coupling between the Fe and Mo sublattices indicates that the ideal saturation magnetization value should be $4\mu_B$, but so far the values obtained from experiments are smaller than the predicted one. Such a result is explained based on the antisite of Fe and Mo arrangements.[11,12] Upon cooling Sr_2FeMoO_6 from high temperatures, a structural phase transition from a cubic $Fm3m$ to a tetragonal $I4/m$ structure occurs at about 400 K.[13] Ba_2FeMoO_6 forms a cubic structure with a space group $Fm3m$. Ba has a larger radius than Sr, so $Sr_{2-x}Ba_xFeMoO_6$ with different Ba contents will have different internal pressures. Recently, Feng *et al.*[14] studied the crystal structure, transport, and magnetic properties of $Sr_{2-x}Ba_xFeMoO_6$, and found the valence transition from Fe^{3+}-Mo^{5+} to Fe^{2+}-Mo^{6+} in the range of $x>1.6$ accompanying metal-insulator transition. In addition, they discussed the relationship between Curie temperature T_C and composition in terms of antisite defects and chemical pressure. Application of high pressure would produce external pressure and modify the structural, electrical, and magnetic properties of materials. So it is meaningful to study the structural sta-

bility and electrical properties in these double perovskite compounds under external pressures. This will be helpful for further understanding the CMR effect in double perovskite compounds. In this work, we have studied the effect of Ba content on the initial magnetization of $Sr_{2-x}Ba_xFeMoO_6$ series and the structural stability and electrical properties under high pressure of the three selected samples in this series.

II. EXPERIMENTS

The polycrystalline samples of $Sr_{2-x}Ba_xFeMoO_6$ were prepared by a traditional solid-state reaction method. The $SrCO_3$, BaO, Fe_2O_3, and MoO_3 powders were mixed and ground with a nominal composition of $Sr_{2-x}Ba_xFeMoO_6$. The mixed powder was then palletized and heated, with intermediate grinding at 1000 °C in Ar for 4 h, 1100 °C and 1125 °C in 1% H_2 in Ar streams for 3 h and 4 h, respectively. The detailed procedure of sample preparation was described elsewhere.[15] The magnetic moment measurements were carried out on Mag Lab equipment. The room temperature x-ray diffraction (XRD) measurement was performed using a Rigaku D/Max-2400 diffractometer with Cu $K\alpha$ radiation. *In situ* high-pressure energy dispersive x-ray diffraction experiments on $Sr_{2-x}Ba_xFeMoO_6$ were carried out in a diamond anvil cell (DAC), with a culet of 480 μm diameter, using synchrotron white radiation at the Beijing Synchrotron Radiation Facility (BSRF).[16] The size of the x-ray spot was 80×80 μm, and the diffraction angle (θ) was 8.776°. The powder of the sample was loaded, together with a suitable amount of Pt powder for internal pressure calibration, into a 300 μm diameter hole in a T301 stainless steel gasket.

The ratio V/V_0 as a function of pressure P for the sample was obtained from the change of the spacing d between lattice planes in the synchrochron x-ray diffraction experiments.

The resistance and capacitance as functions of pressure at room temperature were measured in a DAC with a ZL5 intelligent *LCR* meter at 1 kHz. The techniques used for DAC and measurements were the same as those used previously.[17] The distance between the two molybdenum electrodes is 0.03–0.05 mm. All the samples studied were prepressed under a definite pressure to make a compact sample before the measurement.

III. RESULTS AND DISCUSSION

The structure of the sintered sample was checked by XRD measurement. Figure 1 shows the XRD patterns of the sintered $Sr_{2-x}Ba_xFeMoO_6$ samples at room temperature. These patterns show that the $Sr_{2-x}Ba_xFeMoO_6$ samples form a cubic structure with a space group $Fm3m$ in the x range of 0.2–2 while Sr_2FeMoO_6 forms a tetragonal structure with a space group $I4/mmm$, in consistent with the results in Ref. 14. The lattice parameters are $a=b=5.5709(1)$ Å and $c=7.9011(1)$ Å for Sr_2FeMoO_6 and $a=b=c=8.0678(1)$ Å for Ba_2FeMoO_6. In the cubic samples, the patterns also show that the lattice parameter a increases with increasing Ba content. The lattice parameter at room temperature versus Ba content x is shown in Fig. 2 (open circles for right axis). The error bars are omitted since they are small and difficult to present. No trace of impurity was detected in the measurements. The cubic structure of Ba_2FeMoO_6 was also confirmed through the observations of transmission electron microscopy.

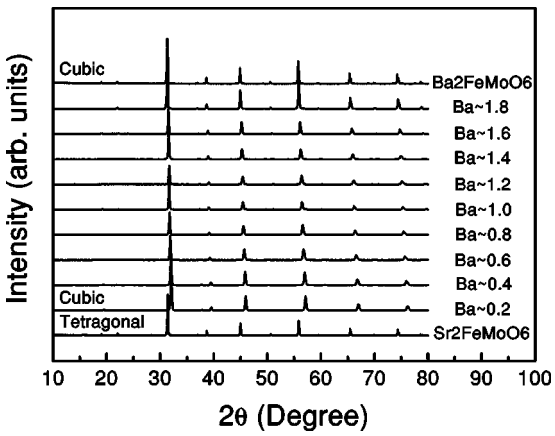

FIG. 1. The powder x-ray diffraction pattern of $Sr_{2-x}Ba_xFeMoO_6$ at room temperature. The $Sr_{2-x}Ba_xFeMoO_6$ form a cubic phase with x in the range of 0.2–2 while the Sr_2FeMoO_6 forms an orthorhombic one.

Figure 3 shows the initial magnetization measurements of the series compounds of $Sr_{2-x}Ba_xFeMoO_6$ measured at 5 K. One can see that the saturation magnetization value of the samples increases and the magnetic field needed for getting the saturation magnetization decreases with the increase of Ba content except for two compositions with $x=1.2$ and 1.4. The saturation magnetization moment of Ba_2FeMoO_6 is nearly $4\mu_B$ per formula unit (f.u.), which is the ideal value for such compounds. Up to date the large magnetization value has not been obtained for bulk Sr_2FeMoO_6; instead smaller values below $3.7\mu_B$/f.u. have been reported. The origin of the smaller experimental value can be explained by the so-called antisite *B*-cation disorder. As is well known, an *A*-site ion plays a very important role in the perovskite structure and its physical properties. A Ba ion is larger than Sr

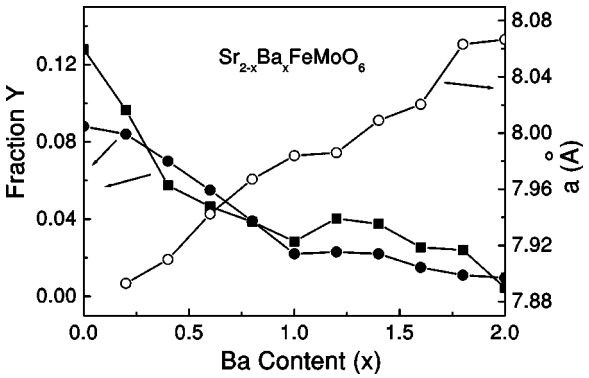

FIG. 2. Open circles for the right axis are the lattice parameter at room temperature versus the Ba content x in the range of 0.2–2; full square dots and full circles for left axis are the fraction y of Fe atoms replaced by Mo atoms versus the Ba content x obtained from saturation magnetization values and Rietveld refinement, respectively.

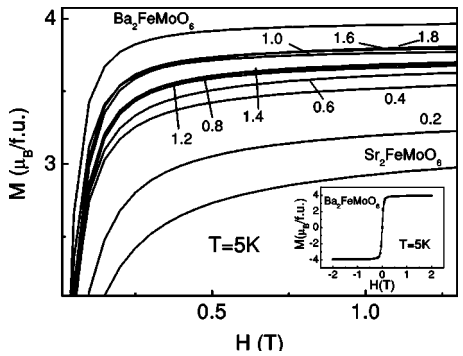

FIG. 3. The initial magnetization of the series compounds of $Sr_{2-x}Ba_xFeMoO_6$ measured at 5 K. The inset is the magnetic hysteresis loop of Ba_2FeMoO_6 at 5 K.

ion. In our experiments, with the increase of substitution of Sr by Ba, the structure and the arrangement of the *B* site become more regular; thus the antisite case of the *B* ions decreases, i.e., the Fe and Mo ions construct a nearly perfect antiferromagnetic configuration. This results in the increase of the saturation magnetic moment value, consistent with the results in Ref. 14. The magnetic hysteresis loop of Ba_2FeMoO_6 at 5 K is shown in the inset of Fig. 3. As is well known, the *B* site ordering is closely related to sample preparation condition, such as heating temperature and treating time.[18,19] It should be pointed out that the saturation magnetization value of Sr_2FeMoO_6 in our experiment is low compared to the reported value, which may be caused by nonoptimal synthesis conditions. Even though, in such a case, the above results show a clear rule that the *B* site ordering is also affected by *A* site atom, such as the atom radius.

If we consider that the Fe and Mo ions have ferrimagnetic configuration and assume the local magnetic moments are $5\mu_B$ and $1\mu_B$ for Fe and Mo ions, respectively, then the ideal saturation magnetic moment can be obtained as $M_S = M_{Fe}\text{-}M_{Mo}$. Thus in the case of antisite occupancy of Mo at Fe positions and Fe at Mo positions, the saturation magnetization can be written as $M_S=(4-8y)\ \mu_B$/f.u.,[11,18] where *y* is the fraction of Fe atoms replaced by Mo atoms. Then $y=0.5$ corresponds to the completely disordered structure. According to this formula and the measured saturation magnetization values, the *y* values corresponding to different *x* for $Sr_{2-x}Ba_xFeMoO_6$ series are calculated and the relationship between *y* and *x* is depicted in Fig. 2 (full square dots for left axis) together with that obtained from Rietveld analyses (full circles for left axis). Again the error bars are omitted due to their small values. It shows that the *B* site ordering increases with the increase of Ba content in the *A* site except for the two compositions with $x=1.2$ and 1.4. The falling short of the two compositions may be caused by the slightly different sintering conditions even though we tried to keep the conditions the same.

Due to the difference of Sr and Ba ionic radii, the substitution of Ba for Sr results in a chemical pressure in the structure. Thus, it is meaningful to study the structural behavior and physical properties of $Sr_{2-x}Ba_xFeMoO_6$ under external pressure. In order to check the structural stability of $Sr_{2-x}Ba_xFeMoO_6$, we performed *in situ* high-pressure energy dispersive x-ray diffraction experiments for three chosen samples (Sr_2FeMoO_6, $SrBaFeMoO_6$, Ba_2FeMoO_6). Figures 4(a) and 4(b) present the patterns of energy dispersive x-ray diffraction of $SrBaFeMoO_6$ and Ba_2FeMoO_6 at room temperature and different pressures, respectively. The results on Sr_2FeMoO_6 has been published elsewhere.[20] The maximum pressures applied are 38.3 and 30.1 GPa for $SrBaFeMoO_6$ and Ba_2FeMoO_6, respectively. From Fig. 4 it can be seen that no structural changes occur in both of the patterns except for a slight shift of peak in the patterns as the pressure increases, showing the slight decrease of the lattice parameters. The weakening of the sample peak intensities at high pressures is due to the sample flowage out of the sample hole, and little broadening of the peaks is caused by the sample thinning and pressure gradients in the sample at high pressures. This indicates that for the two samples no structural transition occurs in the measured pressure range except for some crystal compression under high pressure, which suggests that the crystal structure of $Sr_{2-x}Ba_xFeMoO_6$ is stable in the measured pressure range.

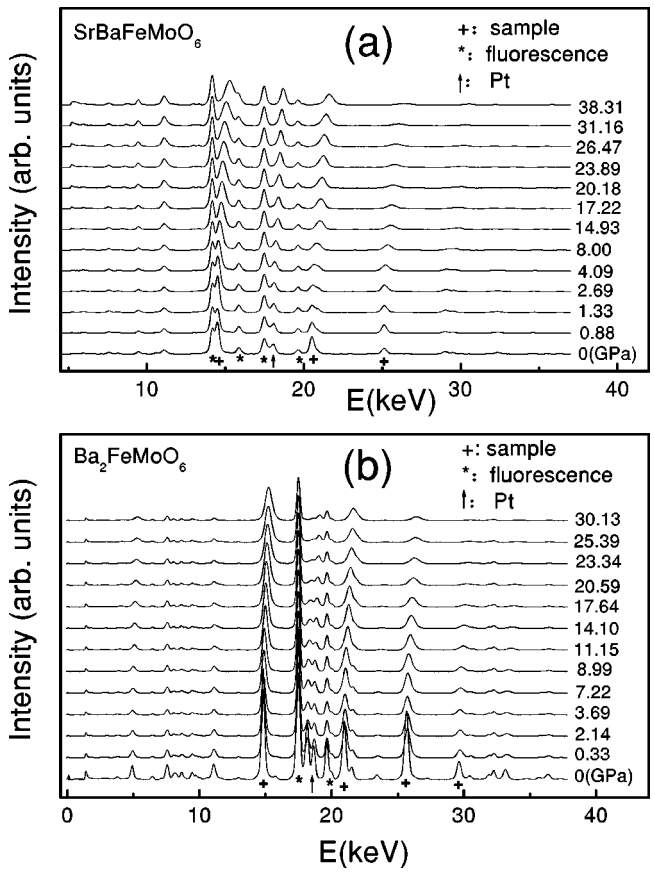

FIG. 4. Energy dispersive x-ray diffraction of $SrBaFeMoO_6$ and Ba_2FeMoO_6 at room temperature and different pressures.

Figure 5 shows the V/V_0-P curves of $SrBaFeMoO_6$ and Ba_2FeMoO_6 at room temperature together with that of Sr_2FeMoO_6 for comparison in the measured pressure range, from which one can see that the volume of the unit cell of each compound decreases with increasing pressure. The experimental data are fitted by the Birch-Murnaghan (BM) equation.[21]

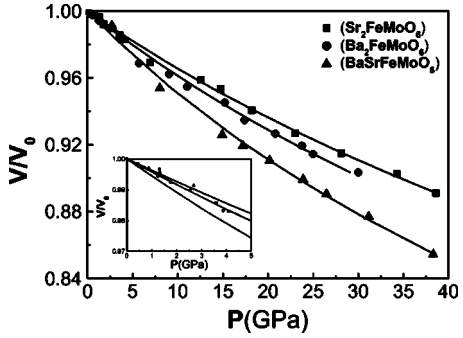

FIG. 5. Fitted V/V_0-P curves of Ba_2FeMoO_6, $SrBaFeMoO_6$, and Sr_2FeMoO_6 at room temperature according to the BM equation. The inset is the enlarged view of the region of 0–5 GPa.

$$P=\frac{3}{2}B_0\left[\left(\frac{V}{V_0}\right)^{-7/3}-\left(\frac{V}{V_0}\right)^{-5/3}\right]\left\{1-\frac{3}{4}(4-B_0')\times\left[\left(\frac{V}{V_0}\right)^{-2/3}-1\right]\right\}.$$

The bulk modulus B_0 are 234, 178, and 266 GPa for Ba_2FeMoO_6, $BaSrFeMoO_6$, Sr_2FeMoO_6, respectively, assuming their first order derivative $B_0'=4$. In order to show clearer features of $V(P)$ in the range of 2–4 GPa, where the anomaly behavior in the resistance and capacitance measurements are described later, the enlarged view is in the inset of Fig. 5. No anomaly can been found in the inset data.

The three samples have high bulk modulus values that are reasonable for the perovskite structures. But there are some differences among the three. As discussed above, the Ba ion is larger than Sr. Table I lists the bond lengths in Sr_2FeMoO_6 and Ba_2FeMoO_6 structures, obtained through the Rietveld analyses of the powder x-ray diffraction patterns of Sr_2FeMoO_6 and Ba_2FeMoO_6 at room temperature. Table I shows that the corresponding bond lengths in Ba_2FeMoO_6 are larger than those in Sr_2FeMoO_6. This may be one possible reason for the experimental result that Sr_2FeMoO_6 has a higher bulk modulus than Ba_2FeMoO_6. As for the $SrBaFeMoO_6$, half of the Ba ions are replaced by smaller Sr ions without changing the symmetry of the crystal structure except for a little shortening of the lattice parameter. Though the cell parameter shortens a little, in order to keep the same symmetry, there are still more vacancies around Sr ions due to its smaller radius. This may be a reason why the $SrBaFeMoO_6$ structure is compressed more easily than Ba_2FeMoO_6 and results in the lowest bulk modulus for $SrBaFeMoO_6$ among the three samples.

TABLE I. The bond lengths in Sr_2FeMoO_6 and Ba_2FeMoO_6 structures, obtained through the Rietveld analyses of x-ray diffraction patterns of Sr_2FeMoO_6 and Ba_2FeMoO_6 at room temperature.

Sr_2FeMoO_6	Bond length (Å)	Ba_2FeMoO_6	Bond length (Å)
Sr-O(1)	2.790(8)	Ba-O	2.852(1)
Sr-O(2)	2.7856(3)		
Fe-O(1)	1.96(2)	Fe-O	2.06(2)
Fe-O(2)	2.00(3)		
Mo-O(1)	1.97(2)	Mo-O	1.97(2)
Mo-O(2)	1.95(3)		

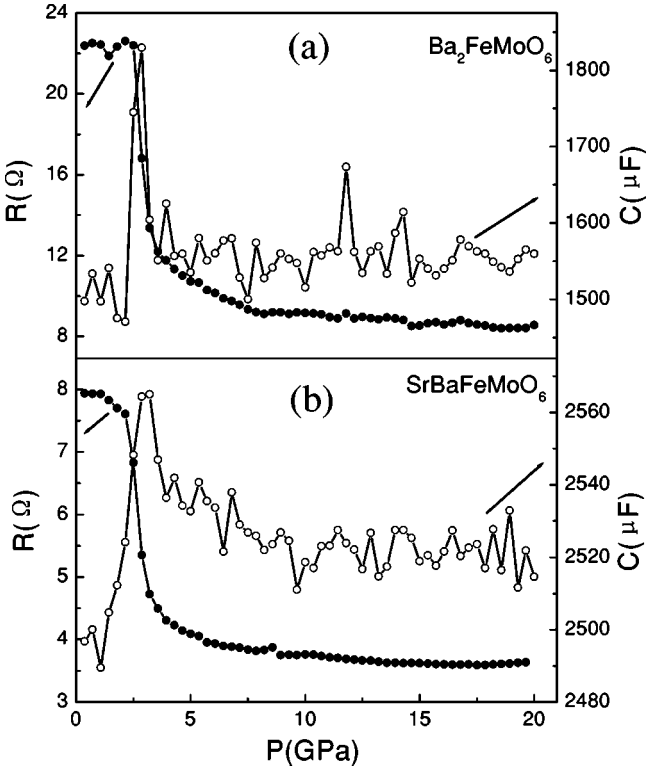

FIG. 6. Pressure dependence of resistance (full circles) and capacitance (open circles) at room temperature for (a) Ba_2FeMoO_6 and (b) $SrBaFeMoO_6$.

The transport behavior of the double perovskite compounds has a very close relationship with preparation conditions. Though the single crystal and thin film form show the metallic behavior,[22,23] the ceramics show metallic, semiconductor, or insulating behavior based on different synthesis conditions.[13] Here we should point out that all the samples we prepared show semiconducting or insulating behavior. Figure 6(a) presents the pressure dependence of the resistance and capacitance for Ba_2FeMoO_6 at room temperature. With increasing pressure, the resistance of the sample remains a constant at first and then drops steeply at about 2.3–3.8 GPa, and decreases slowly to 20 GPa, showing either a crystal or electronic structural transition at about 2.3–3.8 GPa. The capacitance versus pressure was measured simultaneously in the measurement. With increasing pressure, the capacitance rises abruptly also at the same pressure range. Figure 6(b) presents the resistance and capacitance versus pressure for $SrBaFeMoO_6$ at room temperature. Except for a little higher pressure corresponding to the drop in resistance and rise in capacitance, $SrBaFeMoO_6$ shows a similar electrical behavior under pressure to Ba_2FeMoO_6, which is also similar to Sr_2FeMoO_6.[12] All the measurements were carried out on at least three different pieces from one sample. The phenomena in the resistance and capacitance are reversible in the unloading process. Since the sample was prepressed un-

der about 4 GPa, the effect caused by the intergrains on the electrical properties can be neglected. Based on the analyses of the energy dispersive x-ray diffraction results that show no crystal structural change, the remarkable changes in the resistance and capacitance in Figs. 6(a) and 6(b) suggest that there may be an electronic structural change under pressure, which is caused by the compression of the unit cell. As mentioned above, Sr_2FeMoO_6 has a half-metal band structure. The related band structure may be sensitive to the compression of the unit cell caused by high pressure, and the Fe t_{2g} and Mo t_{2g} electrons can be strongly influenced by the change of band structure. The details need to be further studied by other measurements, for example, photoelectron energy spectrum under pressure.

IV. CONCLUSIONS

The effect of Ba content on initial magnetization of $Sr_{2-x}Ba_xFeMoO_6$ series has been investigated. The initial magnetization value increases and lower magnetic field is needed for getting the saturation magnetic moment with the increase of Ba content in the compound. And the antisite of *B* cations becomes less with increasing Ba content. *In situ* high-pressure energy dispersive x-ray diffraction studies for three of the $Sr_{2-x}Ba_xFeMoO_6$ samples have been carried out with synchrotron radiation. No crystal structural transition occurs in the measured pressure range except for the compression of the unit cell, indicating that the structure of the $Sr_{2-x}Ba_xFeMoO_6$ is stable in the measured pressure range. The electrical properties of the samples have also been studied. The steep drop in resistance and the abrupt rise in capacitance observed in the measurements are considered to being caused by the electronic structural transition. The electronic structure transition might be caused by the compression of the unit cell, which results in the changes of the band structure. The equations of state of Ba_2FeMoO_6 and $SrBaFeMoO_6$, are obtained from the V/V_0-P relationship based on the BM equation, and the bulk modulus values are obtained assuming their first order derivative $B_0'=4$.

ACKNOWLEDGMENTS

This work was supported by the National Natural Science Foundation of China (Grants No. 10274099 and No. 50321101) and the State Key Development Project on Fundamental Research (No. 2002CB613301). The *in situ* high-pressure energy dispersive x-ray diffraction experiments were carried out at the Beijing Synchrotron Radiation Facility (BSRF). We thank Professor L. C. Chen, Professor Z. X. Bao, and Professor C. X. Liu for their help with the measurements.

*Corresponding author.

[1] K.-I. Kobayashi, T. Kimura, H. Sawada, K. Terakura, and Y. Tokura, Nature (London) **395**, 677 (1998).

[2] B. García-Landa, C. Ritter, M. R. Ibarra, J. Blasco, P. A. Algarabel, and R. Mahendiran, J. García, Solid State Commun. **110**, 435 (1999).

[3] Y. Moritomo, Sh. Xu, T. Akimoto, A. Machida, N. Hamada, K. Ohoyama, E. Nishibori, M. Takata, and M. Sakata, Phys. Rev. B **62**, 14224 (2000).

[4] J. Lindén, T. Yamamoto, M. Karppinen, H. Yamauchi, and T. Pietari, Appl. Phys. Lett. **76**, 2925 (2000).

[5] A. W. Sleight and J. F. Weicher, J. Phys. Chem. Solids **33**, 679 (1972).

[6] M. Venkatesan, M. Grafoute, A. P. Douvalis, J.-M. Greneche, R. Suryanarayanan, and J. M. D. Coey, J. Magn. Magn. Mater. **242-245**, 744 (2002).

[7] S. E. Lofland, T. Scabarozi, Y. Moritomo, and Sh. Xu, J. Magn. Magn. Mater. **260**, 181 (2003).

[8] A. S. Ogale, S. B. Ogale, R. Ramesh, and T. Venkatesan, Appl. Phys. Lett. **75**, 537 (1999).

[9] Y. Moritomo, H. Kusuya, A. Machida, and T. Akimoto, Jpn. J. Appl. Phys., Part 2 **39**, L360 (2000).

[10] Z. Fang, K. Terakura, and J. Kanamori, Phys. Rev. B **63**, 180407 (2001).

[11] A. S. Ogale, S. B. Ogale, R. Ramesh, and T. Venkatessan, Appl. Phys. Lett. **75**, 537 (1999).

[12] D. Sánchez, J. A. Alonso, M. García-Hernández, M. J. Martínez-Lope, and J. L. Martínez, Phys. Rev. B **65**, 104426 (2002).

[13] O. Chmaissem, R. Kruk, B. Dabrowski, D. E. Brown, X. Xiong, S. Kolesnik, J. D. Jorgensen, and C. W. Kimball, Phys. Rev. B **62**, 14197 (2000).

[14] X. M. Feng, G. H. Rao, G. Y. Liu, W. F. Liu, Z. W. Ouyang, and J. K. Liang, J. Phys.: Condens. Matter **16**, 1813 (2004).

[15] P. Zhao, Z. X. Bao, C. X. Liu, M. Z. Jin, R. C. Yu, and C. Q. Jin, J. High Press. Phys. **16**, 137 (2002).

[16] J. Liu, J. Zhao, R. Z. Che, and Y. Yang, Chinese Science Bulletin **45**, 1659 (2000).

[17] Z. X. Bao, V. H. Schmidt, and F. L. Howell, J. Appl. Phys. **70**, 6804 (1991).

[18] LI. Balcells, J. Navarro, M. Bibes, A. Roig, B. Martínez, and J. Fontcuberta, Appl. Phys. Lett. **78**, 781 (2001).

[19] P. Woodward, R. D. Hoffmann, and A. W. Sleight, J. Mater. Res. **9**, 2118 (1994).

[20] P. Zhao, R. C. Yu, F. Y. Li, Z. X. Liu, M. Z. Jin, and C. Q. Jin, J. Appl. Phys. **92**, 1942 (2002).

[21] L. Gerward, J. Phys. Chem. Solids **46**, 925 (1985).

[22] Y. Tomioka, T. Okuda, Y. Okimoto, R. Kumai, K.-I. Kobayashi, and Y. Tokura, Phys. Rev. B **61**, 422 (2000).

[23] T. Manako, M. Izumi, Y. Konishi, K. I. Kobayashi, M. Kawasaki, and Y. Tokura, Appl. Phys. Lett. **74**, 2215 (1999).